Journal Pre-proof

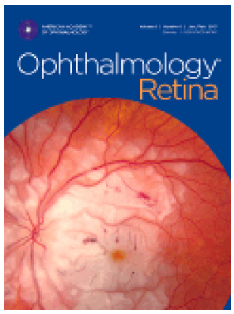

Deep learning to detect optical coherence tomography-derived diabetic macular edema from retinal photographs: a multicenter validation study

Xinle Liu, PhD, Tayyeba K. Ali, MD, MS Preeti Singh, Ami Shah, MD, Scott Mayer McKinney, MS, Paisan Ruamviboonsuk, MD, Angus W. Turner, MSc, FRANZCO, Pearse A. Keane, MD, FRCOphth, Peranut Chotcomwongse, MD, Variya Nganthavee, MD, Mark Chia, MBBS, MMed, Josef Huemer, MD, FEBO, Jorge Cuadros, OD, PhD, Rajiv Raman, MBBS, MS, Greg S. Corrado, PhD, Lily Peng, MD, PhD, Dale R. Webster, PhD, Naama Hammel, MD, Avinash V. Varadarajan, MS, Yun Liu, PhD, Reena Chopra, BSc, Pinal Bavishi, BE

PII: S2468-6530(22)00001-X

DOI: https://doi.org/10.1016/j.oret.2021.12.021

Reference: ORET 1142

To appear in: *Ophthalmology Retina*

Received Date: 13 September 2021

Revised Date: 9 November 2021

Accepted Date: 29 December 2021

Please cite this article as: Liu X., Ali T.K., Singh P., Shah A., McKinney S.M., Ruamviboonsuk P., Turner A.W., Keane P.A., Chotcomwongse P., Nganthavee V., Chia M., Huemer J., Cuadros J., Raman R., Corrado G.S., Peng L., Webster D.R., Hammel N., Varadarajan A.V., Liu Y., Chopra R. & Bavishi P., Deep learning to detect optical coherence tomography-derived diabetic macular edema from retinal photographs: a multicenter validation study, *Ophthalmology Retina* (2022), doi: https://doi.org/10.1016/j.oret.2021.12.021.

Deep learning to detect optical coherence tomography-derived diabetic macular edema from retinal photographs: a multicenter validation study

Xinle Liu, PhD[1†], Tayyeba K. Ali, MD[2,3†], Preeti Singh, MS[1], Ami Shah, MD[2], Scott Mayer McKinney, MS[1], Paisan Ruamviboonsuk, MD[4], Angus W. Turner, MSc, FRANZCO[5,6], Pearse A. Keane, MD, FRCOphth[7], Peranut Chotcomwongse, MD[4], Variya Nganthavee, MD[4], Mark Chia, MBBS, MMed[5,7], Josef Huemer, MD, FEBO[7], Jorge Cuadros, OD, PhD[8], Rajiv Raman, MBBS, MS[9], Greg S. Corrado, PhD[1], Lily Peng, MD, PhD[1], Dale R. Webster, PhD[1], Naama Hammel, MD[1]*, Avinash V. Varadarajan, MS[1], Yun Liu, PhD[1], Reena Chopra, BSc[1,7]*, Pinal Bavishi, BE[1]

[1] Google Health, Google LLC, Mountain View, CA, USA

[2] Work done at Google Health via Advanced Clinical, Deerfield, IL, USA

[3] Present affiliation: California Pacific Medical Center, Department of Ophthalmology, San Francisco, CA

[4] Department of Ophthalmology, Rajavithi Hospital, College of Medicine, Rangsit University, Bangkok, Thailand

[5] Lions Outback Vision, Lions Eye Institute, Nedlands, Western Australia, Australia

[6] University of Western Australia, Perth, Western Australia, Australia

[7] NIHR Biomedical Research Centre for Ophthalmology, Moorfields Eye Hospital NHS Foundation Trust and UCL Institute of Ophthalmology, London, United Kingdom

[8] EyePACS Inc., Santa Cruz, CA, USA

[9] Shri Bhagwan Mahavir Vitreoretinal Services, Sankara Nethralaya, Chennai, India

[†] Equal contribution

* Co-corresponding authors

Meeting presentation

Part of this work has been presented as an abstract at ARVO Annual Meeting 2020.

Financial support

Google LLC funded this study, and participated in the design of the study, conducting the study, data collection, data management, data analysis, interpretation of the data, preparation, review and approval of the manuscript.

Conflicts of interest

P.R. is a consultant for Roche, Novartis, and Bayer. P.A.K. has acted as a consultant for DeepMind, Roche, Novartis, and Apellis and is an equity owner in Big Picture Medical. He has received speaker fees from Heidelberg Engineering, Topcon, Allergan, and Bayer. He is supported by a Moorfields Eye Charity Career Development Award (R190028A) and a UK Research & Innovation Future Leaders Fellowship (MR/T019050/1). J.H. served on advisory boards for Roche. He has received speaker fees from Bayer and Zeiss. J.C. is CEO of EyePACS, Inc.. X.L., P.S., S.M.M., G.S.C., L.P., D.R.W., N.H., A.V.V., Y.L., R.C., and P.B. are employees of Google LLC and own Alphabet stock.

Running head

Deep learning to predict OCT-derived labels of DME from CFP

Address for reprints

Naama Hammel, MD, Google Health, Google LLC, 1600 Amphitheatre Parkway, Mountain View, CA 94043, USA. nhammel@google.com

Reena Chopra, BSc, Google Health, Google LLC, 6 Pancras Square, Kings Cross, London N1C 4AG, UK. reenac@google.com

Keywords

Diabetic Retinopathy, Diabetic Macular Edema, Deep Learning, Optical Coherence Tomography, Artificial Intelligence

Word count

3848 words

Acknowledgments

The authors would like to thank Ehsan Rahimy, MD, Siva Balasubramanian, MD, PhD, Ilana Traynis, MD, Ali Zaidi, MD, and all the graders for guideline iteration and labeling retinal images; Mahvish Nagda, MS, Derek Wu, BS, Jieying Luo, PhD, Roy Lee, BS, Anita Misra B. Tech, Richa Tiwari, PhD, Fred Hersch, MBBS, MPH, Rajroshan Sawhney, BE, Yan Zhen Tan, LLB, Warisara Pattanapongpaiboon, MD, Vaibhav Shah, DNB, for technical and logistical support; Divleen Jeji, MD, MBA and Craig Mermel, MD, PhD for their feedback on the manuscript; and the Google Health labeling software infrastructure team for their assistance.

Abstract

Purpose

To validate the generalizability of a deep learning system (DLS) that detects diabetic macular edema (DME) from two-dimensional color fundus photography (CFP), where the reference standard for retinal thickness and fluid presence is derived from three-dimensional optical coherence tomography (OCT).

Design

Retrospective validation of a DLS across international datasets.

Participants

Paired CFP and OCT of patients from diabetic retinopathy (DR) screening programs or retina clinics. The DLS was developed using datasets from Thailand, the United Kingdom (UK) and the United States and validated using 3,060 unique eyes from 1,582 patients across screening populations in Australia, India and Thailand. The DLS was separately validated in 698 eyes from 537 screened patients in the UK with mild DR and suspicion of DME based on CFP.

Methods

The DLS was trained using DME labels from OCT. Presence of DME was based on retinal thickening or intraretinal fluid. The DLS's performance was compared to expert grades of maculopathy and to a previous proof-of-concept version of the DLS. We further simulated integration of the current DLS into an algorithm trained to detect DR from CFPs.

Main Outcome Measures

Superiority of specificity and non-inferiority of sensitivity of the DLS for the detection of center-involving DME, using device specific thresholds, compared to experts.

Results

Primary analysis in a combined dataset spanning Australia, India, and Thailand showed the DLS had 80% specificity and 81% sensitivity compared to expert graders who had 59% specificity and 70% sensitivity. Relative to human experts, the DLS had significantly higher specificity ($p=0.008$) and non-inferior sensitivity ($p<0.001$). In the UK dataset the DLS had a specificity of 80% ($p<0.001$ for specificity > 50%) and a sensitivity of 100% ($p=0.02$ for sensitivity > 90%).

Conclusions

The DLS can generalize to multiple international populations with an accuracy exceeding experts. The clinical value of this DLS to reduce false positive referrals, thus decreasing the burden on specialist eye care, warrants prospective evaluation.

Introduction

Diabetic macular edema (DME) is characterized by retinal thickening and an accumulation of intraretinal fluid (IRF) caused by abnormal vascular permeability and leakage in diabetic retinopathy and diabetes mellitus, and is a leading cause of blindness among working-aged adults.[1,2] Prompt detection and treatment of DME is imperative to stabilize vision.[3]

Diabetic eye screening programs utilize colour fundus photography (CFP) for detection of diabetic retinopathy (DR) and DME. For DME, the presence of hard exudates (HE) near the fovea is used as a surrogate marker for the presence of fluid. However, this marker alone is an imperfect indicator of DME and has limited specificity and sensitivity.[4,5,6]

Clinical testing via three-dimensional optical coherence tomography (OCT) is increasingly recognized as the reference standard for detection of DME.[7] Clinical trials investigating DME therapies have relied on OCT-derived central retinal thickness as an inclusion criteria and clinical endpoint.[8,9] Another important marker of DME activity on OCT is the presence of intraretinal fluid (IRF), which may gauge response to treatment.[10] Despite the advantage of OCT for reliable diagnosis and classification of DME, this modality remains unavailable in many parts of the world due to its high cost and need for expert interpretation,[11] resulting in ongoing reliance on CFP for DME screening.

Deep learning, a type of artificial intelligence, has been used for computational detection of DR and DME from CFP.[12–15] These deep learning systems (DLSs) are typically trained using CFP with HE-labels and are unlikely to address the sensitivity and specificity gaps. To improve upon expert performance, our group previously reported a DLS that predicted OCT-derived DME labels using only CFP as input (the “DME-DLS”).[16] Other groups have similarly evaluated feasibility of systems that predict OCT-derived central retinal thickness using a CFP input and obtained promising results.[17]

This is the first study of its kind to generalize a DLS aimed at predicting OCT-derived ground truth using CFP as input in multiple, independent screening populations. The performance of the DME-DLS was compared to both expert grading of CFP and the previously reported version of the DLS. Additionally, we analyzed the ability of the DLS in detecting center-involving DME (ci-DME) with definitions based on retinal thickening and IRF presence. As a secondary outcome, the DLS performance for detecting the presence of OCT-based DME irrespective of location was evaluated. To better understand the potential impact of improved DME screening in the context of broader DR screening, we further evaluated the net effect of replacing the DME component of a previously published and extensively validated Krause et. al DLS that detects both DR and DME using conventional grading guidelines.[18,19,20]

Methods

Study data were obtained from multiple sources. These data were collected with the participant's consent and/or de-identified in accordance with local regulatory requirements (e.g., HIPAA) and/or reviewed by the institution's Ethics Committee or IRB prior to our receipt of the dataset. The study adhered to the tenets of the Declaration of Helsinki.

Datasets

Development datasets

Our DLS was developed using 1,167,791 retrospectively collected paired single-field CFP and OCT images from four sites in three countries: Thailand (1,299 images from Lerdsin Hospital and 7,072 from Rajavithi Hospital), the UK (1,156,142 images from Moorfields Eye Hospital), and the US (3,278 images from Alameda County Health System) (Table S1). All images were collected from diabetic patients except for the UK dataset, which consisted of a wide range of retinal pathology. Data were divided randomly, by patient, into train (98.8%) and tune (1.2%) sets, with the ratio based on an empirical estimation of necessary tuning versus training dataset sizes. The train set came from Thailand Lerdsin (100%), Thailand Rajavithi (68%), and the UK (99.3%), while the tune set was gathered from Thailand Rajavithi (32%), the UK (0.7%) and the US (100%). Some datasets were used exclusively for training or tuning to help assess inter-dataset generalization during tuning, thus their ability to generalize to new datasets.

Validation datasets

Validation of the DLS was performed on independent datasets, comprising patients with diabetes from institutions in Australia, India, Thailand and the UK. Datasets from Australia and India were external validation sets. The validation dataset from Thailand was from the same institution as the developmental set; however, it was from a different temporal period

and consisted solely of a screening population (compared to retina clinic patients). The UK dataset was an internal validation dataset from the same institution and an overlapping time period (though without patient duplication) (Table 1).

Definitions, image acquisition, and grading

Definition of OCT-based DME

DLS performance was evaluated using two separate definitions of DME: one based on retinal thickening and the second on IRF presence; each definition was further divided into ci-DME and DME (combined ci-DME and non-center involving [nci-DME]).

For retinal thickening, device- and gender-specific thresholds were used to define ci-DME in ETDRS zone 1/central subfield thickness (CST) in all datasets (Table S2).[3,21–23] For IRF presence, ci-DME was defined as fluid present within ETDRS zone 1. Similarly, nci-DME was defined as retinal thickening or IRF occurring solely in zones 2–9.[24] The retinal thickening based ci-DME definition was used for primary analysis; all other definitions were used for secondary analysis. Further details of defining DME, OCT retinal thickness acquisition and OCT grading of fluid presence can be found in the Supplementary Methods S1.

CFP grading for comparison to DLS

To provide a baseline comparison for the DLS, experienced graders labeled CFP in the validation set for DR severity and for the presence and location of HE within 1500 µm of the foveal center. DR level was based on the International Clinical Diabetic Retinopathy Disease Severity Scale[25] and presence of HE, reflecting clinical practice in DR screening programs. Further details on grading CFPs and image quality guidelines are provided in the Supplementary Methods S1.

Table 2 describes the availability of ground truths and expert grades for comparison in the validation datasets.

Deep learning system

Development

The DME-DLS was trained similarly to the proof-of-concept version,[16] with some significant upgrades to aid generalization. The DME-DLS is a deep convolutional neural network trained with TensorFlow.[27] The DLS takes CFP as input and simultaneously outputs predictions for thickness-based ci-DME, IRF-based ci-DME, and thickness-based DME (inclusive of both ci-DME and nci-DME). While OCT provided the ground truth labels, the actual OCT images were never seen by the DLS during training or validation (Figure 1A). To improve performance, the DLS was developed using multi-task learning with the following co-trained tasks: subretinal fluid presence, prediction of sex, and prediction of age. To aid generalization, this version of the DME-DLS was also trained on the large UK development dataset, with automated labels generated using a previously described segmentation DLS.[28] The current model was trained to predict the volume of fluid output by the segmentation DLS instead of fluid presence alone and it used the EfficientNet-B5 architecture[29] to train on the much larger dataset in a reasonable amount of time. Further details on the DLS design are available in Supplementary Methods S2.

Evaluation

To enable comparison with expert grades, the output of the DLS was thresholded to produce a binary result: DME present or absent. As the Australia, India and Thailand datasets consisted of a screening population where the pre-test probability for presence of DME would be lower, high-specificity operating points were chosen, with separate operating points for ci-DME (thickness and IRF presence) and DME (thickness) outputs. Operating points were selected to maximize specificity on the Thailand and US tune sets, subject to the

constraint that the 95% confidence lower bound of DME-DLS sensitivity was at most 10% lower than the expert graders. The same operating points were used for the aggregated analysis of all three datasets as well as for each individual country's dataset. Since the UK dataset contained data from a pre-screened population with evidence of mild DR and a suspicion of DME, the pre-test probability for presence of DME would be higher, and so a separate high-sensitivity operating point was chosen with 95% confidence lower bound sensitivity of 90%. All operating points were pre-selected before evaluating the model on the validation datasets (Figure 1B).

We further simulated integration of this DME-DLS into another previously validated DLS,[18] with the originally described DLS being referred to as the Krause et al. DLS henceforth. The Krause et al. DLS detects DR and DME and was developed on an independent dataset of CFP using the presence of HE as labels for DME. Our DME-DLS was used to replace the DME detector in the Krause et al. DLS without modifying the DR component (Figure S1). Using the adjudicated Indian dataset, we then compared the original and modified version of the Krause et al. DLS for detecting patients with vision-threatening DR (VTDR), defined as severe non-proliferative DR, proliferative DR, or ci-DME (retinal thickening) in at least one eye.

Statistical analysis

For pre-specified primary analyses, the performance of the DLS was compared with experts, specifically testing superiority of specificity and non-inferiority of sensitivity (at a 10% margin) for detection of ci-DME (thickening) on the aggregation of Australia, India, and Thailand validation sets. Superiority comparisons for specificity were two-sided McNemar tests,[30] while non-inferiority comparisons for sensitivity with a pre-specified margin of 10% were Wald tests.[31] Since there were multiple graders, we adjusted for the clustered nature of the data using Obuchowski's method for paired binomial proportions.[32,33] Confidence intervals for sensitivities and specificities were calculated using the exact Clopper-Pearson interval.

We further conducted receiver operating characteristic (ROC) analysis to evaluate the DLS both in isolation and in comparison to the previously reported version of the DLS. Non-parametric confidence intervals on the area under the curve (AUC)-ROC were computed with DeLong's method.[34]

Secondary analysis evaluated DLS performance when compared to experts on a per-dataset level (Australia, India and Thailand). We also analyzed DLS performance for detection of DME defined by fluid presence, DME irrespective of location, and when restricted to mild-to-moderate DR, where ground truth was available. On the UK dataset, we tested for sensitivity of > 90% and specificity of > 50% using an exact one-sided binomial test.

Results

The DME-DLS was validated on independent, screening datasets from Australia, India and Thailand. Additionally, the DME-DLS was validated in a cohort of patients from the UK screening program referred specifically for maculopathy based on CFP. The characteristics of the cohorts are provided in Table 2. The rate of ci-DME was higher in the India dataset (21%) compared to the other 3 datasets (3–5%). After excluding ungradable images, the DLS was validated on 3574 images.

DME based on retinal thickening

Our primary analysis evaluated the DME-DLS against a reference standard of ci-DME based on retinal thickening in a combined cohort of the Australia, India, and Thailand datasets and compared it to experts grading maculopathy on CFP. The DME-DLS had a specificity of 80% and a sensitivity of 81% compared to expert specificity of 59% and sensitivity of 70%. The DME-DLS had superior specificity ($p=0.008$) and non-inferior sensitivity ($p<0.001$), reducing false positives by 51%. Exploratory analysis revealed the DME-DLS also had superior sensitivity ($p=0.014$) (Table 3).

Per-dataset, the DME-DLS's specificities (vs human experts) for the Australia, India, and Thailand datasets were 86% (vs 57%; $p=0.03$), 77% (vs 44%; $p<0.001$) and 66% (vs 78%; $p=0.20$), respectively; the corresponding sensitivities were 71% (vs 66%, $p=0.007$ for non-inferiority), 84% (vs 72%, $p=0.002$) and 100% (vs 77%, $p=0.013$) (Table 3).

We also compared our DME-DLS's ci-DME detection performance with a previously reported, non-generalized, proof-of-concept version of this DLS (Figure 2A).[16] The current DME-DLS had an AUC of 0.88 compared to 0.80 for the proof-of-concept DLS. For the Australia, India, and Thailand datasets individually, the AUCs for the DME-DLS (vs the

proof-of-concept version) were 0.86 (vs 0.73), 0.89 (0.74), 0.96 (0.93), respectively. The performance was consistent when restricted to eyes with mild-to-moderate DR (Figure S2) and when subgrouped by gender (Figure S3).

For the UK dataset, the DME-DLS had an AUC of 0.96 (vs 0.82 for the proof-of-concept DLS), a specificity of 88% and a sensitivity of 89%. At the prespecified high-sensitivity threshold, the DME-DLS had a specificity of 80% ($p<0.001$ for specificity >50%) and a sensitivity of 100% ($p=0.02$ for sensitivity >90%) (Figure 2B). The DME-DLS reduced false positives by 80% from 661 to 129, while detecting all 37 eyes with ci-DME on OCT.

Besides ci-DME, we evaluated the DME-DLS against a reference standard of DME (based on retinal thickening) anywhere in the macula (Figure S4). The DME-DLS specificities (vs human experts) for the Australia, India and Thailand datasets were 93% (vs 69%), 87% (vs 55%) and 70% (vs 86%) respectively; the corresponding sensitivities were 56% (vs 60%), 76% (vs 72%) and 90% (vs 65%), respectively.

DME based on intraretinal fluid presence

When assessing DLS performance against the expert graded reference standard in detecting DME defined by IRF, similar trends in performance were noted (Figure 2C-D). In the Australia and India validation datasets, at the pre-specified threshold, the DLS specificities (vs human experts) were 92% (vs 68%) and 67% (vs 44%), respectively; the corresponding sensitivities were 64% (vs 63%) and 89% (vs 71%), respectively. Additionally, the DLS had an AUC of 0.86 and 0.88 compared to 0.74 and 0.77, respectively, for the previously reported proof-of-concept DLS (Figure 2C). There was no significant impact on performance of the DLS when the reference standard was expanded to IRF presence anywhere in the macula (Figure S3D).

For the UK dataset, the DLS had a sensitivity of 56% and a specificity of 95%. At the prespecified high-sensitivity threshold the DLS had a sensitivity of 94% ($p=0.032$ for sensitivity > 90%) and a specificity of 52% ($p<0.001$ for specificity > 45%) (Figure 2D). The DLS reduced false positives from 520 to 247, while missing only 9 of 162 eyes with ci-DME on OCT. None of the 9 eyes had ci-DME based on retinal thickening. The DLS had an AUC of 0.88 compared to 0.72 for the proof-of-concept DLS.

Confusion matrices of DLS and expert grades for ci-DME defined by retinal thickening and IRF presence, where available, in all four validation sets is presented in Figure S7.

Evaluation in the context of DLS-based DR screening

Both original and modified versions of the Krause et al. DLS had similar sensitivities for detecting VTDR ($p<0.001$ for non-inferiority): 93% vs 92%, respectively. The specificity of the modified DLS was significantly higher than the specificity of the original (69% vs 60%, $p=0.03$). Thus, the modified Krause et al. DLS had 22% lower false positives for VTDR and 8% fewer VTDR referrals, all without loss in sensitivity (Figure 3).

Qualitative analysis

Finally, we qualitatively analyzed randomly selected instances where the DLS did better or worse compared to retina specialists. Figure 4A shows an eye where HE are present near the fovea whereas the corresponding OCT shows an absence of ci-DME (thickening or fluid). This is a canonical example of false positive reduction achieved by the DLS. Figure 4B illustrates an example where the DLS detects a clear case of ci-DME without any HE on the corresponding CFP. Additional examples of false positive and false negative cases can be found in Figures S5 and S6, respectively. Figure 4C-D demonstrate examples of DLS false negative and false positive, respectively. In both cases the visibility in the macular region appears to be compromised, which could be a potential cause for the DLS errors.

Discussion

We present a DME-DLS that interprets CFP to provide a DME status that is significantly more specific than experts grading CFP for HEs, while retaining non-inferior sensitivity. We also achieved significantly higher performance when compared to a previously reported proof-of-concept version of the DME-DLS. Our results generalized across sites in four countries with diverse populations, to different DME definitions, location of DME, and to subgroups of patients with varying severities of DR, including the mild-to-moderate DR patient population for whom the screening tool will be most applicable. Use of a DLS similar to the one we present here holds particular clinical relevance, as diagnosis within screening centers rely heavily upon CFP, which can be less specific and lead to unnecessary referrals.

In the UK, OCT surveillance clinics have recently been established as an intermediary stage to refine referrals between screening and specialist centers for patients with mild DR and suspected DME,[35] as false positive rates can be as high as 86%.[6] This is an important cohort to consider as specialty review is generally not required and rescreening at 12–24 months is recommended in the absence of DME.[36] While OCT surveillance clinics can be more cost effective relative to direct referral from screening to a specialist center,[35] it may not always be logistically feasible, and continues to place significant burden on patients to attend appointments and on expert clinicians to interpret the OCT. Therefore, using the UK validation set, we simulated implementation of the DLS as an ancillary second reader after initial screening has occurred in a cohort of patients that might be referred to the OCT surveillance clinic to identify false positives for DME presence. Our results suggest that the DLS could reduce unwarranted referrals by 80%, while not missing a single positive case.

In resource-constrained healthcare systems such as in Thailand, the Krause et al. DR grading system has been effective at providing real-time results to patients.[37] However,

human-centered evaluation observed concerns from both nurses and patients of a false positive result leading to the additional travel burden for referral follow-up, the cost of missing work, and the emotional strain due to a positive result.[37] In addition, false positives place significant burden on already overwhelmed secondary care systems. Similarly, the Australian dataset was from an Aboriginal community clinic, where the DR screening occurs with CFP in many geographically isolated communities without specialist services. By reducing false positives for DME, high costs as well as logistical and cultural barriers are avoided when attempting to coordinate follow-up care. For the India validation set, we simulated the application of integrating this highly-specific DME detection DLS for automated DR screening. In this analysis, we were able to reduce false positive VTDR referrals by 22% and overall VTDR referrals by 8% with no statistically significant loss in sensitivity.

We demonstrate that the DLS can detect DME within 3000 μm of the foveal center and ci-DME affecting the central 500 μm. Anti-vascular endothelial growth factor drugs and steroid implants have demonstrated efficacy in improving visual acuity in patients with ci-DME[38] and delaying treatment can lead to suboptimal visual gains.[39] Nci-DME is also of significance as it may be a precursor to visually significant ci-DME and should be monitored for risk of progression.[40] In these patients, focal laser treatment may be indicated to reduce leakage and stabilize visual acuity.[41,42] Furthermore, our DLS can detect DME defined by thickening or IRF presence. Although these definitions are correlated, we found that only 20–66% of eyes with ci-DME, defined by either thickening or IRF, demonstrated both. Our DLS could be used to triage patients—prioritizing those who meet one or both definitions.

The performance of the DLS was robust when assessing different degrees of DR severity. DME can be found in eyes at any DR severity level and can run an independent course to DR.[43] In patients with mild or moderate DR, there is a risk of missing DME: Wang et al. found over 1 in 4 cases were missed when using CFP labels compared to an OCT reference standard.[5] Exploratory analysis revealed our DLS to also have a higher sensitivity. Figure 4B

and Figure S6 illustrate instances with no hard exudates at the macula but with ci-DME on OCT that was correctly detected by the DLS. Such cases would have been missed if relying upon conventional CFP grading. This could be studied more rigorously with larger and prospectively planned datasets in the future.

Prior work from our group has shown that the features around the fovea are most relevant for the proof-of-concept version of our DME-DLS.[16] Explainability techniques such as heat maps have been applied, highlighting areas highly correlated with the DLS prediction.[44] Compared to the Krause et al. DLS, which focused on HE locations in the whole 45 degree CFP, the DME-DLS primarily focused on the fovea, leading to superior performance. Another explainability technique in prior work used CycleGAN,[45] a type of Generative Adversarial Network that transforms negative cases into positive cases and vice versa, to visualize the changes in CFP features that are necessary for the transformation. This approach observed that transformations from DME to no-DME (or vice versa) involved the removal (or addition) of hard exudates and a darkening (or brightening) of the foveal region.[44] Consistent with these findings, from qualitative analysis, we found that a proportion of incorrect predictions for the current DLS may be attributed to CFP artifacts such as poor contrast or macular shadows that might result from suboptimal pupil dilation (Figure 4C–D). In the future, improved interpretability of the DLS could provide an opportunity for clinicians to learn from and better diagnose DME directly from CFPs.

In terms of aggregate performance (Australia, India, and Thailand datasets), the DLS met the primary endpoint of superior specificity and non-inferior sensitivity using a pre-specified operating point. However, we note that on a per-dataset level, the ROC curves suggest that the operating points could be further calibrated on a per-site basis to achieve a better trade-off between sensitivity and specificity that accounts for local preferences and resource constraints. Applicable trade-offs are likely to be dependent on local resource constraints and the desired sensitivity. The shape of the ROC curve also varies between the sites, which

421 is likely due to differences in the population distribution. Future work could explore selecting
422 the ideal operating point for a given setting.
423
424 To be clinically applicable and robust, we developed and validated the DLS on images
425 acquired from multiple manufacturers using gender and device-specific thresholds. However,
426 due to site-specific differences in OCT devices and scan protocols, the reference standard
427 for IRF in the secondary analyses differed across datasets in terms of the number of B-
428 scans and area imaged (fovea vs full volumes). Further studies may help understand how
429 these changes in reference standard impact final performance. Furthermore, future work
430 could explore the robustness of the DLS when compared to various thickness thresholds.
431 For example, in the UK, NICE guidelines require point thickness of ≥400 μm in the central
432 subfield to start treatment. A DLS that can identify different levels of ci-DME could more
433 effectively prioritize patients that would be eligible for treatment.

434 Conclusion

435 This study demonstrates that the DME-DLS can generalize to multiple international
436 populations with an accuracy exceeding both experts and a previous proof-of-concept
437 version of the system. As the prevalence of diabetes is increasing, resulting in more
438 individuals requiring DR screening,[46] DLS systems are likely to play a significant role in
439 assisting clinicians to ensure timely grading and referrals with both high sensitivity and
440 specificity.[47] We believe our DLS has most clinical applicability in resource-constrained
441 settings to reduce false positive referrals from screening. Another advantage of our DLS is
442 the ability to triage patients depending on the type of DME, such as ci-DME and nci-DME, as
443 well as thickness and fluid-based definitions. Future work should explore the clinical utility of
444 the DME-DLS through prospective evaluation.

References

1. Cheung N, Mitchell P, Wong TY. Diabetic retinopathy. The Lancet 2010;376:124–136. Available at: http://dx.doi.org/10.1016/s0140-6736(09)62124-3.

2. Zhang X, Saaddine JB, Chou C-F, et al. Prevalence of Diabetic Retinopathy in the United States, 2005-2008. JAMA 2010;304:649. Available at: http://dx.doi.org/10.1001/jama.2010.1111.

3. Baker CW, Glassman AR, Beaulieu WT, et al. Effect of Initial Management With Aflibercept vs Laser Photocoagulation vs Observation on Vision Loss Among Patients With Diabetic Macular Edema Involving the Center of the Macula and Good Visual Acuity: A Randomized Clinical Trial. JAMA 2019;321:1880–1894.

4. Mackenzie S, Schmermer C, Charnley A, et al. SDOCT imaging to identify macular pathology in patients diagnosed with diabetic maculopathy by a digital photographic retinal screening programme. PLoS One 2011;6:e14811.

5. Wang YT, Tadarati M, Wolfson Y, et al. Comparison of Prevalence of Diabetic Macular Edema Based on Monocular Fundus Photography vs Optical Coherence Tomography. JAMA Ophthalmology 2016;134:222. Available at: http://dx.doi.org/10.1001/jamaophthalmol.2015.5332.

6. Wong RL, Tsang CW, Wong DS, et al. Are we making good use of our public resources? The false-positive rate of screening by fundus photography for diabetic macular oedema. Hong Kong Med J 2017;23:356–364.

7. Virgili G, Menchini F, Murro V, et al. Optical coherence tomography (OCT) for detection of macular oedema in patients with diabetic retinopathy. Cochrane Database Syst Rev 2011:CD008081.

8. Nguyen QD, Brown DM, Marcus DM, et al. Ranibizumab for diabetic macular edema:

results from 2 phase III randomized trials: RISE and RIDE. Ophthalmology 2012;119:789–801.

9. Diabetic Retinopathy Clinical Research Network, Wells JA, Glassman AR, et al. Aflibercept, bevacizumab, or ranibizumab for diabetic macular edema. N Engl J Med 2015;372:1193–1203.

10. Kim BY, Smith SD, Kaiser PK. Optical coherence tomographic patterns of diabetic macular edema. Am J Ophthalmol 2006;142:405–412.

11. World Health Organization. World Report on Vision. World Health Organization; 2019. Available at: https://www.who.int/publications/i/item/9789241516570.

12. Ting DSW, Cheung CY-L, Lim G, et al. Development and Validation of a Deep Learning System for Diabetic Retinopathy and Related Eye Diseases Using Retinal Images From Multiethnic Populations With Diabetes. JAMA 2017;318:2211–2223. Available at: [Accessed April 13, 2021].

13. Bellemo V, Lim ZW, Lim G, et al. Artificial intelligence using deep learning to screen for referable and vision-threatening diabetic retinopathy in Africa: a clinical validation study. The Lancet Digital Health 2019;1:e35–e44. Available at: [Accessed April 13, 2021].

14. Nielsen KB, Lautrup ML, Andersen JKH, et al. Deep Learning–Based Algorithms in Screening of Diabetic Retinopathy: A Systematic Review of Diagnostic Performance. Ophthalmology Retina 2019;3:294–304. Available at: [Accessed April 13, 2021].

15. Abràmoff MD, Lou Y, Erginay A, et al. Improved Automated Detection of Diabetic Retinopathy on a Publicly Available Dataset Through Integration of Deep Learning. Invest Ophthalmol Vis Sci 2016;57:5200–5206.

16. Varadarajan AV, Bavishi P, Ruamviboonsuk P, et al. Predicting optical coherence tomography-derived diabetic macular edema grades from fundus photographs using deep

493 learning. Nat Commun 2020;11:130.

494 17. Arcadu F, Benmansour F, Maunz A, et al. Deep Learning Predicts OCT Measures of
495 Diabetic Macular Thickening From Color Fundus Photographs. Invest Ophthalmol Vis Sci
496 2019;60:852–857. Available at: [Accessed April 13, 2021].

497 18. Krause J, Gulshan V, Rahimy E, et al. Grader Variability and the Importance of
498 Reference Standards for Evaluating Machine Learning Models for Diabetic Retinopathy.
499 Ophthalmology 2018;125:1264–1272.

500 19. Ruamviboonsuk P, Krause J, Chotcomwongse P, et al. Deep learning versus human
501 graders for classifying diabetic retinopathy severity in a nationwide screening program. npj
502 Digital Medicine 2019;2. Available at: http://dx.doi.org/10.1038/s41746-019-0099-8.

503 20. Gulshan V, Rajan RP, Widner K, et al. Performance of a Deep-Learning Algorithm vs
504 Manual Grading for Detecting Diabetic Retinopathy in India. JAMA Ophthalmol 2019.
505 Available at: http://dx.doi.org/10.1001/jamaophthalmol.2019.2004.

506 21. Brown JC, Solomon SD, Bressler SB, et al. Detection of diabetic foveal edema: contact
507 lens biomicroscopy compared with optical coherence tomography. Arch Ophthalmol
508 2004;122:330–335.

509 22. Sadda SR, Tan O, Walsh AC, et al. Automated detection of clinically significant macular
510 edema by grid scanning optical coherence tomography. Ophthalmology 2006;113:1187.e1–
511 12.

512 23. Abràmoff MD, Lavin PT, Birch M, et al. Pivotal trial of an autonomous AI-based
513 diagnostic system for detection of diabetic retinopathy in primary care offices. NPJ Digit Med
514 2018;1:39.

515 24. Friedman SM, Almukhtar TH, Baker CW, et al. Topical nepafenec in eyes with
516 noncentral diabetic macular edema. Retina 2015;35:944–956.

25. Wilkinson CP, Ferris FL, Klein RE, et al. Proposed international clinical diabetic retinopathy and diabetic macular edema disease severity scales. Ophthalmology 2003;110:1677–1682. Available at: http://dx.doi.org/10.1016/s0161-6420(03)00475-5.

26. Public Health England. NHS Diabetic Eye Screening Programme: Overview of patient pathway, grading pathway, surveillance pathways and referral pathways. 2017. Available at: https://assets.publishing.service.gov.uk/government/uploads/system/uploads/attachment_data/file/648658/Diabetic_Eye_Screening_pathway_overviews.pdf.

27. Abadi M, Agarwal A, Barham P, et al. TensorFlow: Large-Scale Machine Learning on Heterogeneous Distributed Systems. arXiv [csDC] 2016. Available at: http://arxiv.org/abs/1603.04467.

28. De Fauw J, Ledsam JR, Romera-Paredes B, et al. Clinically applicable deep learning for diagnosis and referral in retinal disease. Nat Med 2018;24:1342–1350.

29. Tan M, Le QV. EfficientNet: Rethinking Model Scaling for Convolutional Neural Networks. arXiv [csLG] 2019. Available at: http://arxiv.org/abs/1905.11946.

30. Fagerland MW, Lydersen S, Laake P. Recommended tests and confidence intervals for paired binomial proportions. Stat Med 2014;33:2850–2875.

31. Liu J-P, Hsueh H-M, Hsieh E, Chen JJ. Tests for equivalence or non-inferiority for paired binary data. Stat Med 2002;21:231–245.

32. Obuchowski NA. On the comparison of correlated proportions for clustered data. Stat Med 1998;17:1495–1507.

33. Yang Z, Sun X, Hardin JW. A note on the tests for clustered matched-pair binary data. Biom J 2010;52:638–652.

34. DeLong ER, DeLong DM, Clarke-Pearson DL. Comparing the areas under two or more correlated receiver operating characteristic curves: a nonparametric approach. Biometrics

1988;44:837–845.

35. Leal J, Luengo-Fernandez R, Stratton IM, et al. Cost-effectiveness of digital surveillance clinics with optical coherence tomography versus hospital eye service follow-up for patients with screen-positive maculopathy. Eye 2019;33:640–647.

36. Public Health England. NHS Diabetic Eye Screening Programme: Grading definitions for referable diseases. 2012. Available at: https://assets.publishing.service.gov.uk/government/uploads/system/uploads/attachment_data/file/582710/Grading_definitions_for_referrable_disease_2017_new_110117.pdf.

37. Beede E, Baylor E, Hersch F, et al. A Human-Centered Evaluation of a Deep Learning System Deployed in Clinics for the Detection of Diabetic Retinopathy. In: *Proceedings of the 2020 CHI Conference on Human Factors in Computing Systems*. CHI '20. New York, NY, USA: Association for Computing Machinery; 2020:1–12. Available at: [Accessed March 31, 2021].

38. Schmidt-Erfurth U, Garcia-Arumi J, Bandello F, et al. Guidelines for the Management of Diabetic Macular Edema by the European Society of Retina Specialists (EURETINA). Ophthalmologica 2017;237:185–222.

39. Boyer DS, Nguyen QD, Brown DM, et al. Outcomes with As-Needed Ranibizumab after Initial Monthly Therapy: Long-Term Outcomes of the Phase III RIDE and RISE Trials. Ophthalmology 2015;122:2504–13.e1.

40. Bressler NM, Diabetic Retinopathy Clinical Research Network, Miller KM, et al. Observational study of subclinical diabetic macular edema. Eye 2012;26:833–840. Available at: http://dx.doi.org/10.1038/eye.2012.53.

41. Scott IU, Danis RP, Bressler SB, et al. Effect of focal/grid photocoagulation on visual acuity and retinal thickening in eyes with non-center-involved diabetic macular edema. Retina 2009;29:613–617.

566 42. Perente I, Alkin Z, Ozkaya A, et al. Focal laser photocoagulation in non-center involved
567 diabetic macular edema. Med Hypothesis Discov Innov Ophthalmol 2014;3:9–16.

568 43. Keenan TDL, Johnston RL, Donachie PHJ, et al. United Kingdom National
569 Ophthalmology Database Study: Diabetic Retinopathy; Report 1: prevalence of centre-
570 involving diabetic macular oedema and other grades of maculopathy and retinopathy in
571 hospital eye services. Eye 2013;27:1397–1404.

572 44. Narayanaswamy A, Venugopalan S, Webster DR, et al. Scientific Discovery by
573 Generating Counterfactuals using Image Translation. arXiv [csCV] 2020. Available at:
574 http://arxiv.org/abs/2007.05500.

575 45. Zhu J-Y, Park T, Isola P, Efros AA. Unpaired Image-to-Image Translation using Cycle-
576 Consistent Adversarial Networks. arXiv [csCV] 2017. Available at:
577 http://arxiv.org/abs/1703.10593.

578 46. Cho NH, Shaw JE, Karuranga S, et al. IDF Diabetes Atlas: Global estimates of diabetes
579 prevalence for 2017 and projections for 2045. Diabetes Res Clin Pract 2018;138:271–281.

580 47. Wong TY, Sabanayagam C. Strategies to Tackle the Global Burden of Diabetic
581 Retinopathy: From Epidemiology to Artificial Intelligence. Ophthalmologica 2020;243:9–20.

582

Figure Legends

Figure 1. Study design. A: The deep learning system (DLS) was trained to take color fundus photography (CFP) as input to predict optical coherence tomography (OCT)-derived diabetic macular edema (DME) presence, using datasets from Thailand, the UK and the US. B: The DLS was evaluated for non-inferiority of sensitivity and superiority of specificity, and compared to experts on datasets from Australia, India, and Thailand. The DLS was separately evaluated on a dataset from the UK. Given the difference in patient population (DR screening in Australia, India and Thailand, vs. pre-screened diabetes patients with a higher likelihood of DME in the UK), these datasets were separately analyzed. Both the DLS and expert graders saw only the CFP. The reference standard was based on measurements from OCT.

Figure 2. Receiver operating characteristic curves of the DME-DLS, a previously reported proof-of-concept version of the DLS (not generalized), and experts for detecting ci-DME. The threshold for the DLS was pre-specified. The experts graded the presence of hard exudates within 1500 µm. A) Comparison of performance of both DLSs and experts in a combined cohort of the screening datasets from Australia, India and Thailand consisting of eyes with mild or worse DR. ci-DME was defined by central subfield thickness exceeding OCT device specific threshold. B) Comparison of performance of both DLSs in the separate UK validation dataset consisting of patients referred from screening for DME. C) Comparison of performance of both DLSs and experts in the Australia and India datasets on eyes with mild or worse DR. ci-DME was defined by the presence of intraretinal fluid in the central subfield. D) Comparison of performance of both DLSs in the UK validation dataset. Intraretinal fluid presence grades were not available for the Thailand dataset.

Figure 3: Effect of replacing the DME component of the Krause et al. DLS with the DME-DLS presented in this paper on the India dataset. The Krause et al. DLS (left) and the modified Krause et al. DLS (right) have identical rates of severe+DR compared with the

609 adjudicated ground truth (center). Yet, the dark red flow (left) shows the substantially larger
610 number of DME categorizations made by the original Krause et al. DLS compared to the
611 brighter red flow (right) for the modified Krause et al. DLS (i.e. reduced number of false
612 positives by the modified DLS); the sensitivity remains unchanged (as shown by the green
613 bar on the top).

614 **Figure 4. Selected paired CFPs and OCTs for DLS success and failure, as compared with**
615 **retina specialists (RS) grading CFPs.** A) Hard exudates (HE) within 1500 μm, no thickening or
616 fluid on the OCT - detected correctly by the DLS. B) No HE within 1500 μm, thickening and fluid
617 on the OCT - detected correctly by the DLS. C) HE within 1500 μm, thickening and fluid on the
618 OCT - missed by the DLS. D) No HE within 1500 μm, no thickening or fluid on the OCT - false
619 positive reported by the DLS.

Characteristic	Australia	India	Thailand	United Kingdom
Institution	Derbarl Yerrigan Health Service, Perth	Sankara Nethralaya, Chennai	Rajavithi Hospital, Bangkok	Moorfields Eye Hospital, London
Collection dates	July 2013 to October 2020	October 2019 to February 2020	February 2020 to July 2020	August 2014 to September 2018
Population	Diabetic patients presenting for DR screening	Diabetic patients visiting outpatient ophthalmology clinic	Diabetic patients presenting for DR screening	Diabetic patients randomly selected from a cohort referred from the DR screening program for at least one eye with mild DR and maculopathy
Patients	866	168	548	537
Age in years, mean (SD)	54.9 (15.0) n=866	60.0 (8.6) n=168	57.6 (11.2) n=548	55.0 (15.1) n=537
Sex (% female)	52.4% n=454	31.5% n=53	62.2% n=341	41.7% n=224
Eyes (one image per eye)	1692	298	1070	698
Eyes used in analysis after excluding ungradable images, %	90.4% n=1530	98.0% n=292	98.5% n=1054	100.0% n=698
No DR, %	75.6% n=1157	44.2% n=129	87.0% n=917	0.0% n=0
Mild DR, %	3.2% n=49	3.4% n=10	4.0% n=42	100.0% n=698
Moderate DR, %	16.5% n=253	27.7% n=81	6.9% n=73	0.0% n=0
Severe DR, %	1.0% n=15	3.1% n=9	1.3% n=14	0.0% n=0
Proliferative DR, %	3.7% n=56	21.6% n=63	0.8% n=8	0.0% n=0
Central subfield thickness in µm, mean (SD)	238.6 (54.5) n=1530	297.5 (118.8) n=291	270.9 (56.0) n=1054	233.0 (42.5) n=698
ci-DME positive (central subfield thickness ≥ threshold), %	3.8% n=58	21.0% n=61	2.5% n=26	5.3% n=37
ci-DME positive (IRF present), %	11.1% n=166	25.0% n=72	Not available	23.8% n=162
ci-DME positive (central retinal thickening and IRF present), %	3.1% n=46	18.4% n=53	Not available	4.8% n=33
DME positive (retinal thickening ≥ threshold)	13.1% n=200	39.0% n=114	4.6% n=49	Not available

Table 1. Baseline characteristics of the validation datasets from multiple institutions in Australia, India, Thailand, and the United Kingdom. Abbreviations: ci-DME: center-involving diabetic macular edema; DR: diabetic retinopathy; SD: standard deviation; IRF: intraretinal fluid.

Dataset	Imaging device(s) used	Ground truth for primary analysis (ci-DME based on CST)	Ground truth for secondary analysis	Expert DR & DME grades from CFP
Australia	CFP + OCT: 3D OCT-1 Maestro (Topcon Corp., Tokyo, Japan)	Topcon software	1. Thickness-based ci-DME and nci-DME from Topcon software 2. Majority grade by 3 ophthalmologists for IRF-based ci-DME and DME using the full OCT volume	Single grades by a pool of 7 retina specialists
India	CFP: NFC 700 (Crystalvue, Taoyuan City, Taiwan) or NW400 (Topcon Corp., Tokyo, Japan) OCT: Cirrus HD-OCT 500 (Carl Zeiss Meditec, Dublin, CA)	Zeiss software	1. Thickness-based ci-DME and nci-DME from Zeiss software 2. Adjudicated grade by 1 retina specialist and 1 ophthalmologist for IRF-based ci-DME using the OCT report, with the central B-Scan containing the fovea	3-way adjudicated grades by a pool of 18 experts (13 retina specialists, 2 ophthalmologists, 3 optometrists)
Thailand	CFP: VX-10 (Kowa, Tokyo, Japan) OCT: Spectralis (Heidelberg Engineering, Heidelberg, Germany)	Heidelberg software	1. Thickness-based ci-DME and nci-DME from Heidelberg software 2. IRF grades not available	Single grades by a pool of 5 retina specialists
UK	CFP + OCT: 3D OCT-2000 (Topcon Corp., Tokyo, Japan)	Topcon software	1. Thickness-based ci-DME from Topcon software after manual recentering of ETDRS grid to fovea (nci-DME measurements not available) 2. Majority grade by 3 ophthalmologists for IRF-based ci-DME and DME using the full OCT volume	Screening grade, derived by a 3-level grading system[26] using certified retinal graders in the diabetic eye screening program

Table 2. Sources of ground truths and expert grades for comparison in the validation datasets. CFP: color fundus photograph; ci-DME: center-involving diabetic macular edema; CST: central subfield thickness; DR: diabetic retinopathy; DME: diabetic macular edema; ETDRS, Early Treatment Diabetic Retinopathy Study; IRF, Intraretinal Fluid; OCT: optical coherence tomography.

	Combined	Australia	India	Thailand
Number of images	673	373	163	137
Number of patients	457	247	106	104
Number of images positive for ci-DME	145	58	61	26
Model specificity	80%	86%	77%	66%
Grader specificity	59%	57%	44%	78%
95% CI for difference	[5%, 36%]	[3%, 54%]	[22%, 43%]	[-32%, 7%]
p-value for difference	0.008	0.030	<0.001	0.201
Model sensitivity	81%	71%	84%	100%
Grader sensitivity	70%	66%	72%	77%
p-value for non-inferiority	<0.001	0.007	0.002	0.013
95% CI for difference	[2%, 20%]	[-7%, 17%]	[-4%, 26%]	[-6%, 52%]
p-value for difference	0.014	0.402	0.127	0.121

Table 3. DLS sensitivity and specificity compared to expert grades for detecting ci-DME in eyes with at least mild DR. The experts graded for the presence of hard exudates within 1500 µm. ci-DME was defined by central subfield thickness exceeding OCT device specific threshold. Abbreviations: ci-DME, center-involving Diabetic Macular Edema; CI, Confidence Interval

A

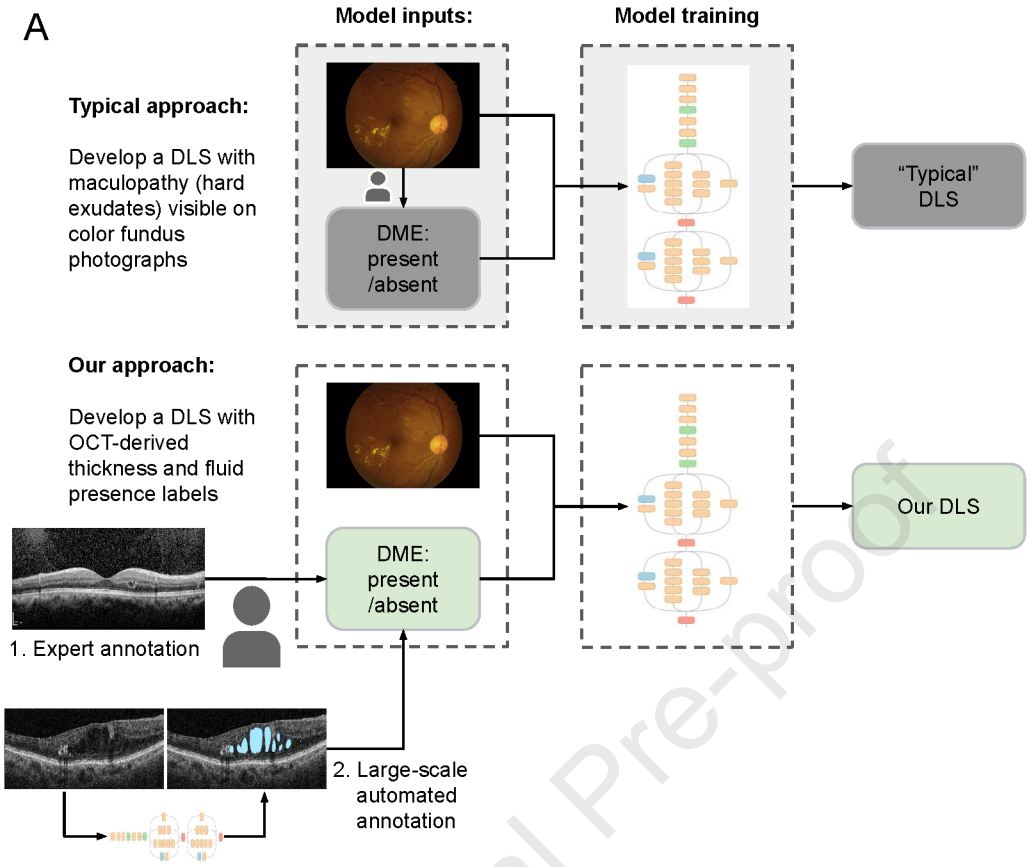

B

DLS development datasets: *Thailand*, *UK and* *US*
DLS validation datasets: *Australia*, *India*, *Thailand and* *UK*

Comparison: Human experts grading for hard exudates within 1500 microns on color fundus photographs

Image for DLS input and expert review:
Color fundus photograph

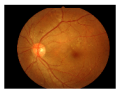

Reference standard:
CST ≥ 300 microns from optical coherence tomography

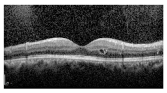

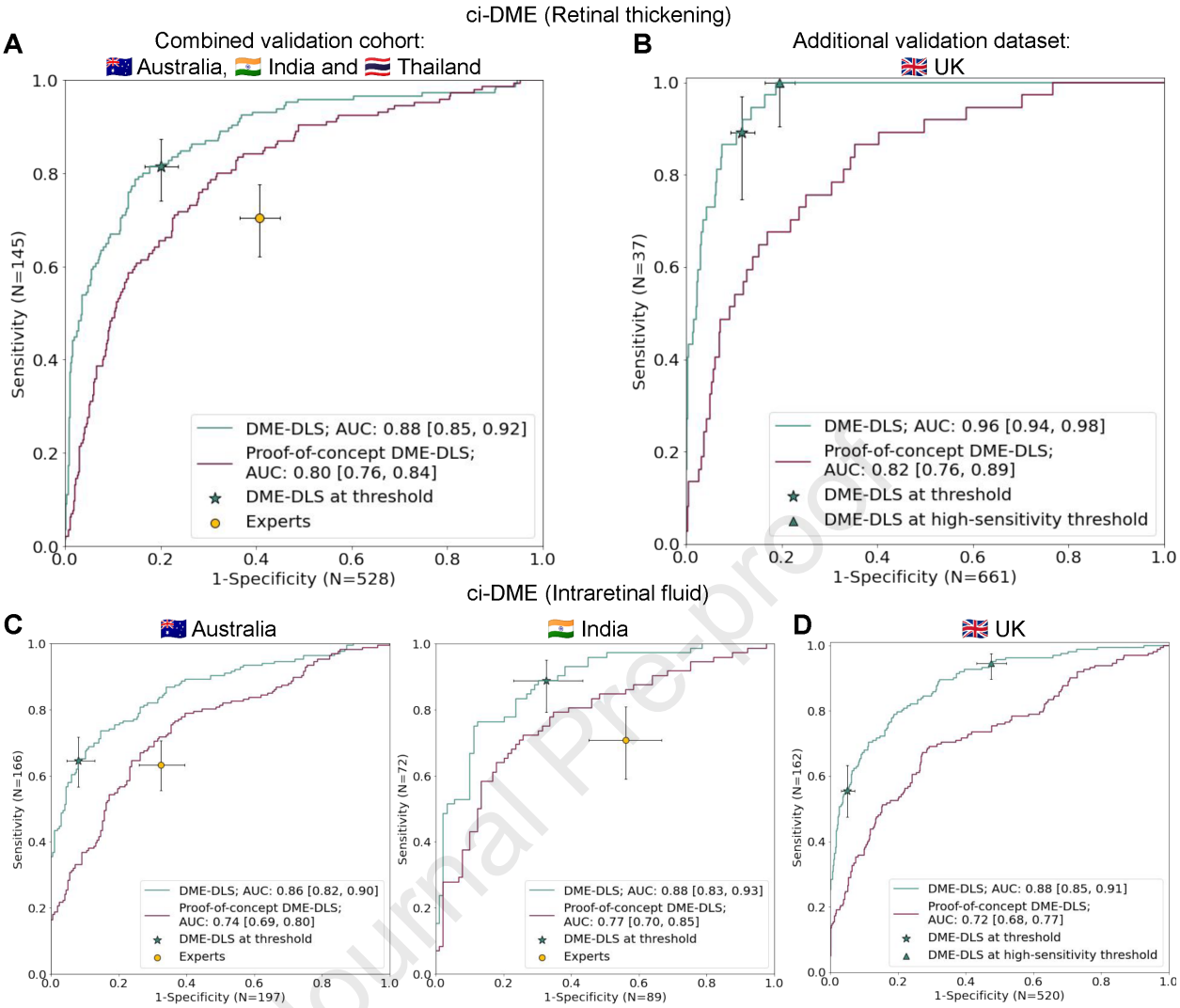

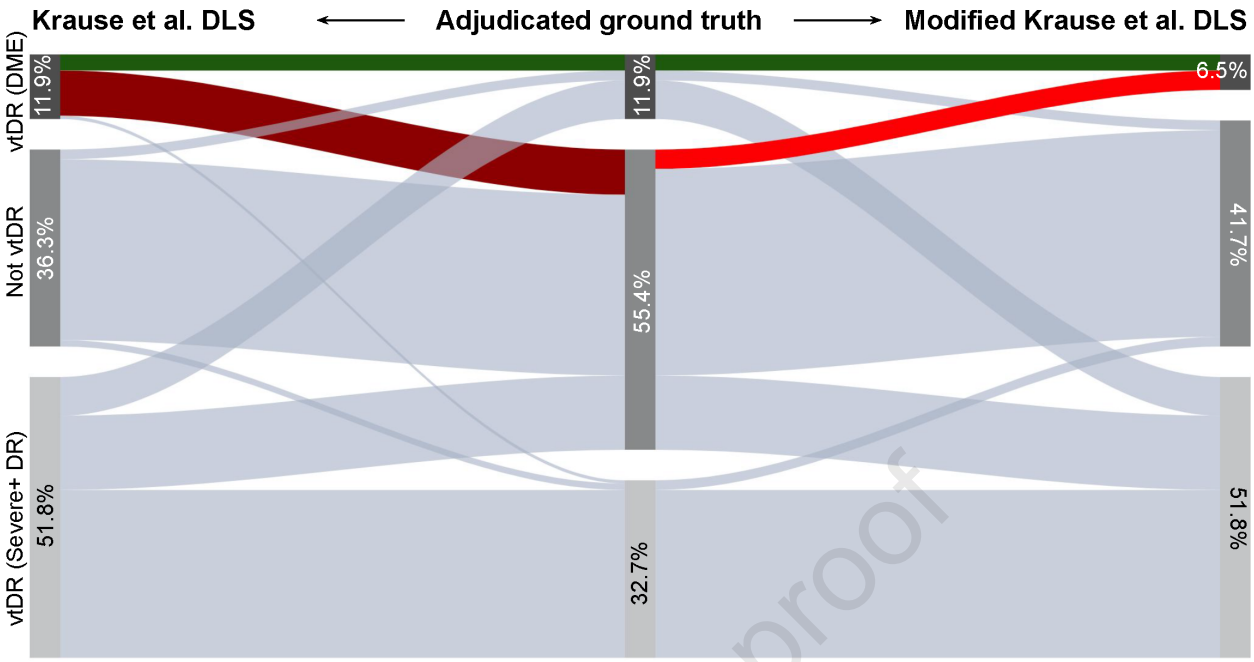

A

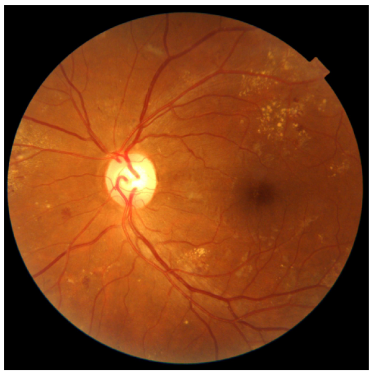

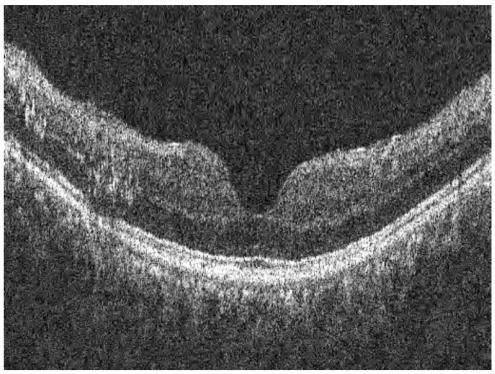

Age: 44
Sex: Male
CST: 179 µm
IRF: No
ci-DME: No

RS: Positive for maculopathy / HE
DLS: Negative for ci-DME

B

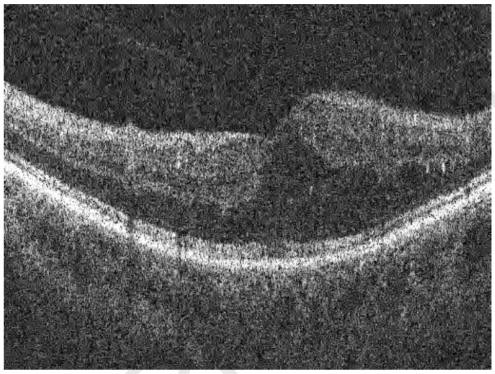

Age: 83
Sex: Female
CST: 353 µm
IRF: Yes
ci-DME: Yes

RS: Negative for maculopathy / HE
DLS: Positive for ci-DME

C

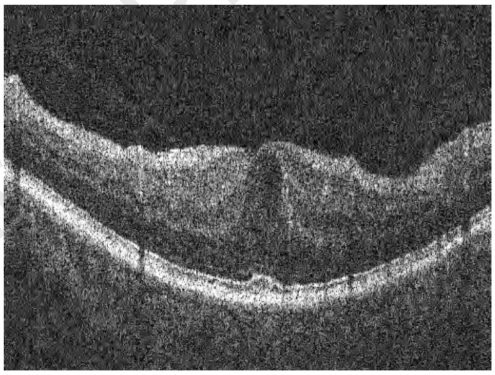

Age: 63
Sex: Male
CST: 361 µm
IRF: Yes
ci-DME: Yes

RS: Positive for maculopathy / HE
DLS: Negative for ci-DME

D

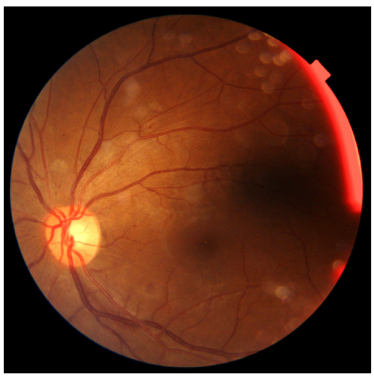

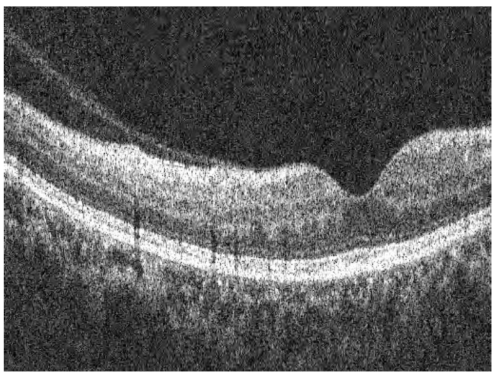

Age: 41
Sex: Female
CST: 267 µm
IRF: No
ci-DME: No

RS: Negative for maculopathy / HE
DLS: Positive for ci-DME

Precis

A deep learning system was trained to predict OCT-derived diabetic macular edema grades from color fundus photographs, and evaluated on international datasets. It achieved a superior specificity and comparable sensitivity to experts grading photographs.